Acta Crystallographica Section D
Biological Crystallography
ISSN 0907-4449

Specific lipid–protein interactions in a novel honeycomb lattice structure of bacteriorhodopsin

Hidenori Sato,[a] Kazuki Takeda,[a] Koji Tani,[a] Tomoya Hino,[a] Tetsuji Okada,[a] Masayoshi Nakasako,[b]† Nobuo Kamiya[b]‡ and Tsutomu Kouyama[a]*

[a]Department of Physics, Graduate School of Science, Nagoya University, Nagoya 464-8602, Japan, and [b]The Institute of Physical and Chemical Research, Wako, Saitama 351-01, Japan

† Present address: Institute for Molecular and Cellular Biosciences, University of Tokyo, Tokyo 113-01, Japan.
‡ Present address: SPring-8 Beamline Facility Division, HARIMA-RIKEN, Kamigori, Ako, Hyogo 678-12, Japan.

Correspondence e-mail: kouyama@bio.phys.nagoya-u.ac.jp

Received 17 August 1998
Accepted 6 April 1999

PDB Reference: bacteriorhodopsin, 1bm1.

In the purple membrane of *Halobacterium salinarium*, bacteriorhodopsin trimers are arranged in a hexagonal lattice. When purple membrane sheets are incubated at high temperature with neutral detergent, membrane vesicularization takes place, yielding inside-out vesicles with a diameter of 50 nm. The vesicular structure becomes unstable at low temperature, where successive fusion of the vesicles yields a crystal which is composed of stacked planar membranes. X-ray crystallographic analysis reveals that the bacteriorhodopsin trimers are arranged in a honeycomb lattice in each membrane layer and that neighbouring membranes orient in opposite directions. The native structure of the trimeric unit is preserved in the honeycomb lattice, irrespective of alterations in the in-plane orientation of the trimer. One phospholipid tightly bound to a crevice between monomers in the trimeric unit is suggested to act as a glue in the formation of the trimer.

1. Introduction

Bacteriorhodopsin (bR), a membrane protein found in the plasma membrane of *Halobacterium salinarium*, functions as a light-driven proton pump. It consists of seven α-helices spanning the membrane roughly perpendicularly and its chromophore, retinal, is bound to the ε-amino group of Lys216 *via* a protonated Schiff base (Stoeckenius *et al.*, 1979; Ebrey, 1993). An interesting property of bR is its self-association into a crystalline array, called purple membrane, under physiological conditions (Blaulock & Stoeckenius, 1971). In purple membrane, bR monomers are associated to form a trimeric structure and the trimers are arranged in a hexagonal lattice (two-dimensional space group $p3$; Henderson *et al.*, 1990). Ten lipid molecules per bR monomer fill the space between the proteins (Kates *et al.*, 1993; Grigorieff *et al.*, 1995). In the absence of the endogenous lipids, bR is unable to form crystalline arrays in dimyristoylphosphatidylcholine (DMPC) bilayers (Sternberg *et al.*, 1992). These facts suggest that the lipid–protein interactions are indispensable for the association of bR monomers into the trimeric structure and the crystalline array.

In order to investigate lipid–protein interactions in higher order structures of bR at atomic resolution, we have developed a new crystallization procedure by which bR crystals containing native lipids are produced. In our previous procedure (Kouyama *et al.*, 1994), a three-dimensional crystal was obtained by concentrating a solution of purple membrane, octylthioglucoside (OTG) and ammonium sulfate at 305 K. At this temperature, purple membrane was transformed into spherical vesicles with a diameter of 50 nm and the vesicles assembled three-dimensionally when the concentration of precipitant reagent exceeded a critical value. The resultant

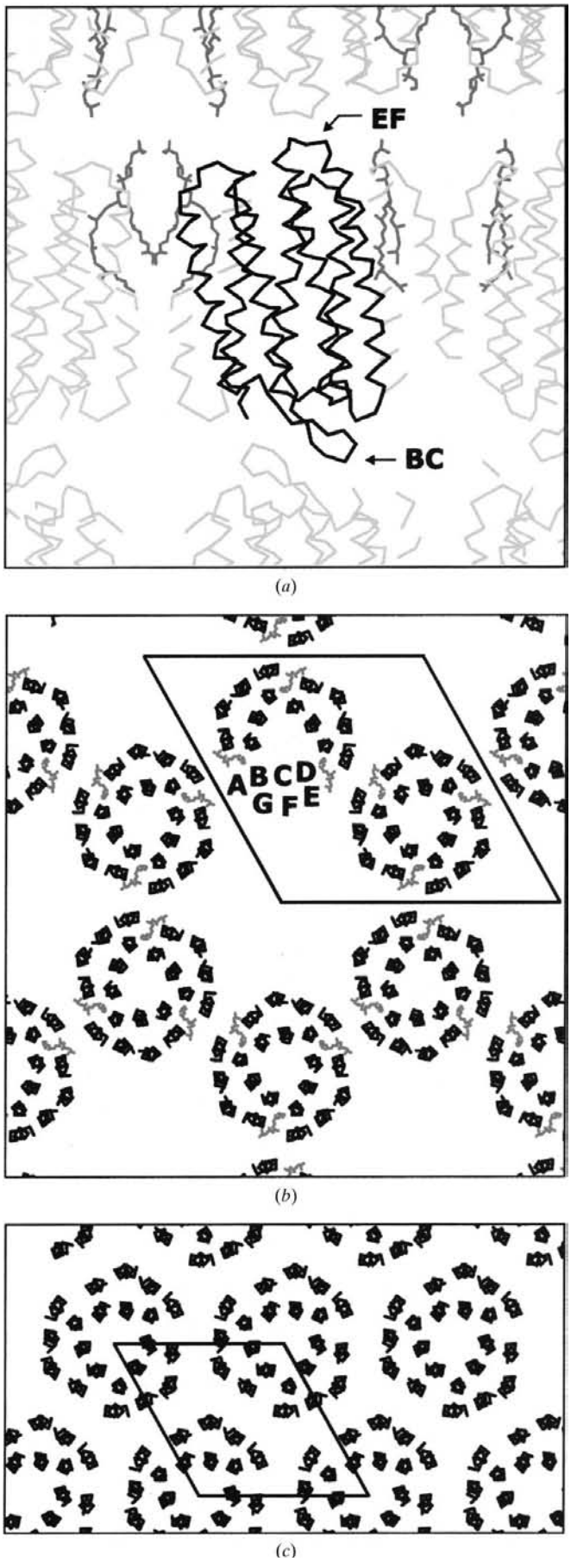

(*a*)

(*b*)

(*c*)

crystal diffracted X-rays to a limited resolution (at best 40 Å), providing little structural information. Recently, another crystal form was produced by concentrating and incubating the spherical vesicles at or below 283 K (Takeda *et al.*, 1998). At this lower temperature, the vesicles tend to fuse with each other and the fused vesicles stack up one on another. As a result of the successive fusion of vesicles, a hexagonal crystal exhibiting birefringence slowly grows. This crystal diffracts X-rays beyond a resolution of 3 Å.

The newly obtained crystal retains native lipids, primarily because crystallization is achieved without solubilizing the protein. Compared with bR crystals obtained using other crystallization procedures (Schertler *et al.*, 1993; Landau & Rosenbusch, 1996), the present crystal has the advantage of providing structural information about the protein–lipid interactions. Here, we focus on a lipid molecule identified in the present crystal structural analysis and discuss its role in the formation of higher order structures of bR.

2. Methods

2.1. Protein purification and crystallization

Purple membrane was isolated from *H. salinarium* JW3 and purified according to an established procedure (Oesterhelt & Stoeckenius, 1974). Prior to crystallization, purple membrane was incubated in a solution containing the neutral detergent Tween 20 for partial delipidation, as previously described (Fukuda *et al.*, 1990). Adjustment of the detergent concentration as well as the incubation period is crucial for successful crystallization. Well ordered crystals were obtained from membranes which were treated with 0.2–0.3% Tween 20 for 30 min at 293 K. The subsequent crystallization procedure is divided into two steps. First, a mixture of 5 mg ml^{-1} purple membrane, 0.25% OTG, 1 *M* ammonium sulfate, 0.16 *M* NaCl, 0.04 *M* sodium citrate (pH 5.2) and 0.02% NaN_3 was incubated at 305 K for 5 d. During this step, vesicularization of purple membrane took place, producing spherical vesicles with a diameter of 50 nm (Kouyama *et al.*, 1994; Denkov *et al.*, 1998). In the next step, sedimentous materials in the mixture were removed by centrifugation at 4000*g* for 30 min. The clear supernatant containing the spherical vesicles was cooled to 278 K and concentrated by vapour diffusion against a reservoir solution containing 2.0 *M* ammonium sulfate and 0.08 *M* sodium citrate. After incubation for a couple of months, hexagonal-shaped crystals grew. Typical crystal dimensions were 0.3 × 0.3 × 0.04 mm.

Figure 1
(*a*) The crystal packing of bR viewed perpendicular to the crystallographic *a* and *c* axes. The C^{α} atoms are depicted in a slab of about 25 Å. The phospholipid found in a crevice between adjacent monomers is drawn in grey. (*b*) The crystal packing viewed from the cytoplasmic side along the *c* axis. The C^{α} atoms in the hydrophobic region near the cytoplasmic surface are depicted in a slab of about 15 Å. (*c*) Arrangement of the bR trimers in native purple membrane (Grigorieff *et al.*, 1996) is shown for comparison.

2.2. Data collection, structural determination and refinements

A single crystal of bR was picked up on a thin quartz plate and the plate was fixed in a glass capillary tube. Diffraction data were collected at 285 K using an imaging plate placed on Sakabe's screenless Weissenberg camera (Sakabe, 1983) at station BL18B of the Photon Factory (Tsukuba, Japan). Indexing and integration of diffraction spots were carried out with *WEIS* (Higashi, 1989). The scaling of diffraction data was performed using *SCALA* and *AGROVATA* from the *CCP*4 program suite (Collaborative Computational Project, Number 4, 1994).

Molecular-replacement analysis was applied for determination of the initial phase using *X-PLOR* (Brünger, 1992*a*). A structural model of bR determined by electron microscopy of purple membrane (Protein Data Bank accession code 2brd; Grigorieff *et al.*, 1996) was used as the search probe. The rotation and translation search was carried out for reflections in the Bragg spacing range 10–4 Å. The best solution in the molecular-replacement analysis gave a high correlation value (0.23) and yielded a crystallographic *R* factor of 0.452 ($R_{\rm free}$ = 0.433) after rigid-body refinement (Brünger, 1992*b*). A final rotation/translation solution is as follows: $\theta_1 = 133.77$, $\theta_2 = 0.11$, $\theta_3 = 29.22^\circ$, $a = 34.9$, $b = 34.7$ and $c = 20.8$ Å. After one round of positional refinement, the *R* factor dropped to 0.403 ($R_{\rm free}$ = 0.421). At this stage, omit $|F_o - F_c|$ Fourier maps were calculated and inspected carefully. The transmembrane helical segments and the retinal chromophore were clearly resolved in the maps. Manual rebuilds were carried out against the $|F_o - F_c|$ electron-density map using the program *XtalView*/*Xfit* (McRee, 1993). After refinement of the manually corrected structural model, an electron-density patch corresponding to one phospholipid was clearly identified. After one phospholipid per bR was introduced, rounds of positional refinement were performed with reflections in the Bragg spacing range 8–3.5 Å. Several residues in the N and *C* termini (Glu1–Gly6 and Ala228–Ser248) were characterized by poor electron density and were not included in the final model. The stereochemistry of the final refined model was checked with the program *PROCHECK* (Laskowski *et al.*, 1993); 89% of the residues are in most favoured regions and 11% are in additional allowed regions of the Ramachandran plot.

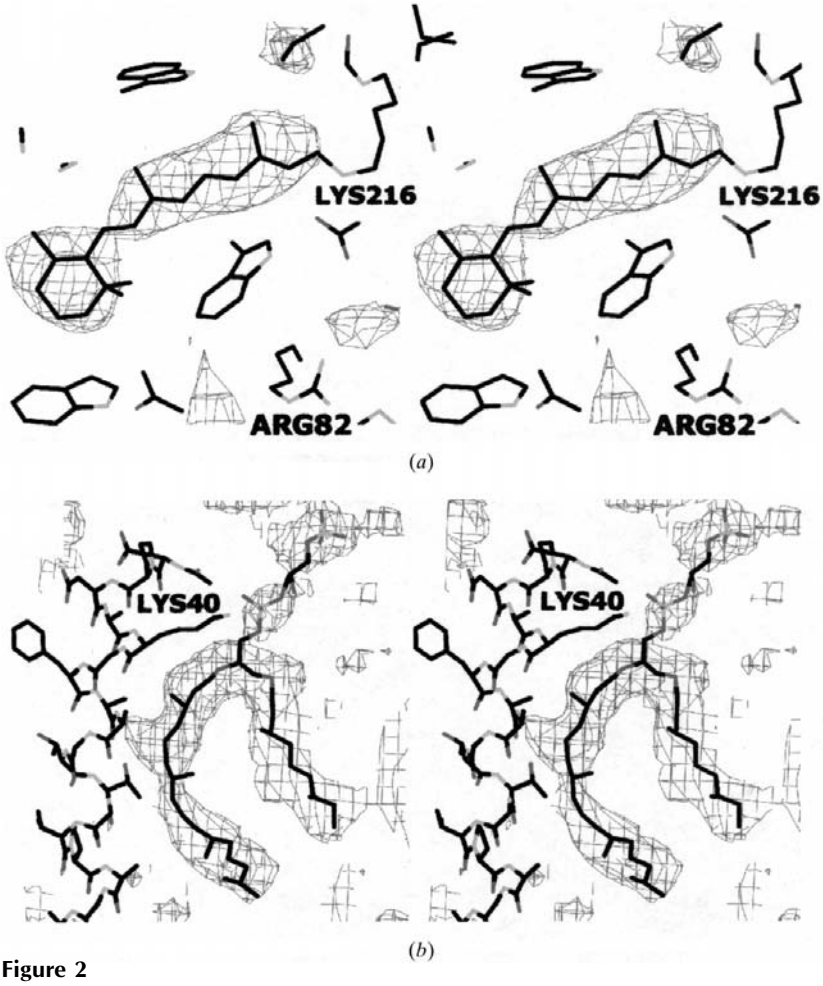

Figure 2
(*a*) Omit map of retinal contoured at 3σ. (*b*) Omit map (1.5σ) of a truncated phospholipid in the crevice between adjacent monomers within the trimeric structure.

3. Results and discussion

3.1. A honeycomb lattice in the new crystal form

The newly obtained crystal belongs to space group *P*622 with unit-cell dimensions $a = b = 104.7$, $c = 114.1$ Å. It is composed of stacked planar membranes which are separated from one another by 57 Å. Neighbouring membrane layers orient in opposite directions and, along the *c* axis, bR molecules in different membrane layers are connected by head-to-head and tail-to-tail interactions (Fig. 1*a*). In each membrane layer, bR trimers are arranged in a honeycomb lattice (Fig. 1*b*). The threefold axis of each trimer coincides with a crystallographic threefold axis, so that the asymmetric unit contains a single monomer. The centre-to-centre distance between adjacent trimers in the honeycomb lattice (60.5 Å) is a little shorter than the corresponding distance in native purple membrane (62.3 Å). The in-plane orientation of each trimer is such that the crevice between monomers in the trimeric unit is near a crystallographic twofold symmetry axis.

3.2. The structure of bR in the light-adapted state

The absorption maximum occurs at 573 nm in the light-adapted crystal and, in the dark, the visible band is blue-shifted by 13 nm with a half-life of 1.3 h at 293 K. These properties are similar to those observed under physiological conditions (Casadio *et al.*, 1980; Fukuda *et al.*, 1990). Since X-ray diffraction data were collected after the crystal was irradiated by

Table 1
Data-collection and final refinement statistics.

Numbers in parentheses are for the highest resolution bin.

Data collection	
Resolution limit (Å)	50–3.5
Data completeness (%)	80.2 (45.2)
Multiplicity	7.4 (4.9)
R_{sym}† (%)	10.3 (15.9)
Refinement	
Resolution limit (Å)	8–3.5
Number of unique reflections	3534 (247)
Number of protein atoms	1717
Number of lipids	1
Final R factor‡ (%)	26.9 (27.2)
R_{free}§	31.1 (36.1)
B factor (Å^2)	
Polypeptide chain	22
Lipid	57
R.m.s. deviations from ideal values	
Bonds (Å)	0.01
Angles (°)	1.4

† $R_{sym} = \sum |I_i - \langle I \rangle| / \sum I_i$, where I_i is the intensity of an individual reflection and $\langle I \rangle$ is the mean intensity obtained from multiple observations of symmetry-related reflections. ‡ $R = \sum(|F_{obs}| - |F_{calc}|) / \sum |F_{obs}|$. § R_{free} is R for 10% randomly omitted reflections which were not used in the refinement calculations.

visible light, the present structural model represents the conformation of the bR isomer containing all-*trans* retinal. This is confirmed by the omit difference map (Fig. 2*a*), in which the retinal chromophore in the *trans* conformation is clearly resolved. The structure of bR was well refined using reflections to a resolution of 3.5 Å (Table 1).

The structures of the seven transmembrane helices are well preserved even after crystallization (Fig. 3*a*). When the present structural model is compared with the probe model (Grigorieff *et al.*, 1996) used in the molecular-replacement analysis, the root-mean-square deviation for all the C^{α} atoms in the helical segments is 0.4 Å. The position of the side-chain groups in the helices is also preserved, except for the residues Trp10, Arg82, Leu97, Phe153 and Glu204 (Fig. 3*a*).

Major structural differences between the probe and the final models are found in the loop regions protruding into the inter-membrane aqueous medium. The loop connecting the *B* and *C* helices folds into antiparallel β-strands in the present model, while it has a distorted conformation in the probe model. The final structure of this loop is nearly identical to that in a recent structural model obtained by electron cryo-microscopic analysis of purple membrane (Kimura *et al.*, 1997). Since the *BC* loop protrudes to a large extent into the aqueous medium, the conformation of this loop would be expected to be sensitive to the environment of the protein. Its structure might be dependent on the degree of hydration of purple membrane, as suggested by the structural difference between the two structural models obtained by electron microscopic analyses (Grigorieff *et al.*, 1996; Kimura *et al.*, 1997).

Another structural difference is found in the conformation of the loop connecting the *E* and *F* helices. This difference is likely to be caused by the stacking of the membrane layers in the present crystal, in which the *EF* loop protrudes toward the adjacent membrane and makes strong contacts with another *EF* loop *via* hydrogen bonds between Ser162 of one monomer and Arg164 of another monomer.

3.3. Lipid–protein interactions

In the present structural analysis, one phospholipid was found in a crevice between adjacent monomers in the trimeric structure (Fig. 2*b*). This lipid molecule is thought to play an essential role in the formation of the trimeric structure of bR. In purple membrane, three species of phospholipid are observed (Kates *et al.*, 1993): diphytanylglycerol (archaeol) having a single phosphatidylglycerol (PG) and its derivatives having an additional charged group [phosphatidylglycero-phosphomethyl (PGP) or phosphatidylglycerosulfate (PGS)]. The omit electron-density map at the present resolution can be fitted by any of these lipid species. In any case, the lipid molecule is attached to the proteins *via* strong electrostatic and van der Waals interactions: (i) the phosphate group of the lipid is in close contact with the ε-amino group of Lys40, which is located at the cytoplasmic end of the *B* helix; (ii) one of its phytanyl chains is tightly packed between the *A* and *B* helices of one monomer and the *D* and *E* helices of the adjacent monomer (Fig. 3*b*). This binding of the lipid to the monomer–monomer interface is similar to that in the probe model (Grigorieff *et al.*, 1996), although there is a significant difference in the conformation of the other phytanyl chain extending outwards from the trimeric unit.

The crystal quality is sensitive to the amount of native lipids remaining in the membrane. The best quality is obtained when the purple membrane is slightly delipidated before crystallization, while no crystal is produced when heavily delipidated purple membrane is used. These results suggest that lipid–protein interactions play a crucial role in crystal growth. Two important results concerning the self-association of bR have previously been reported. Otomo *et al.* (1992) reported that a bR homologue (port-bR) in which Lys40 is substituted by a neutral amino acid is unable to self-associate in the plasma membrane of halobacteria. Sternberg *et al.* (1992) reported that while bR entirely free of the endogenous lipid behaves as a monomer in pure DMPC bilayers, two-dimensional crystalline arrays of bR are formed by the addition of PGP or PGS. Since the phosphate group of PG or its derivative is shown to contact with the ε-amino group of Lys40 in the present crystal structural analysis, these experimental results together suggest strongly that PG or its derivatives act as a glue for the tight association of bR monomers into the trimeric unit.

The bulkiness of the hydrocarbon chain of the archaeol is thought to be an important factor affecting the trimeric formation as well as the optical properties of bR. Pomerleau *et al.* (1995) reported that replacement of the phytanyl chains of the archaeol with alkyl chains results in a large blue shift of the visible absorption band of bR. Since the phytanyl chain is much more bulky than the alkyl chain, such replacement can cause a significant distortion in the conformation of the helical segments near the monomer–monomer interface (the *A* and *B* helices in one monomer and the *D* and *E* helices in the adjacent monomer), which would in turn alter the protein

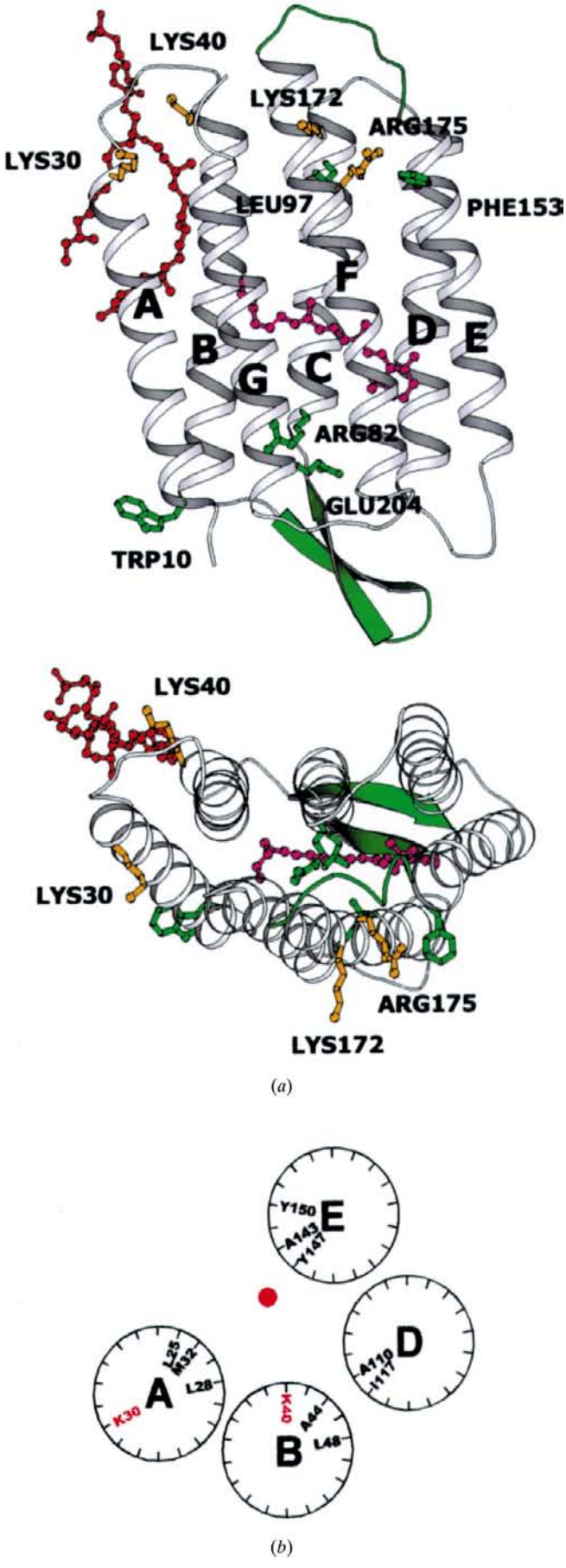

conformation around the retinal chromophore. In Fig. 3(*b*), amino-acid residues contacting with the hydrocarbon chains *via* van der Waals interactions are indicated in black. In the extracellular leaflet of the membrane, these helical segments are closely associated with each other and there is no space to accommodate a lipid between them. This trimeric unit architecture is identical to that seen in the native purple membrane. This similarity explains why the optical properties of the present crystal are very similar to those observed for native purple membrane, irrespective of the presence of detergent molecules.

Structural analyses of purple membrane have indicated that two lipid molecules per bR are immobilized in the central region of the trimeric unit (Grigorieff *et al.*, 1996). However, these lipid molecules are not clearly identified in the present crystal. This is probably because these lipids are partially replaced by detergent molecules. Nonetheless, the angle between the principal axis of the monomer and the membrane normal does not change by more than 0.2° during crystallization. This implies that the lipid molecule in the crevice between the adjacent monomers is more important for the formation of the trimeric structure than the lipid molecules confined to the central region of the trimer.

3.4. Organizational forces in the honeycomb lattice

The mutual orientation of neighbouring bR trimers in the honeycomb lattice (Fig. 1*b*) is completely different from that in native purple membrane (Fig. 1*c*). An interesting question arises as to how the in-plane orientation of the bR trimer is determined in the honeycomb lattice, since no direct contact exists between neighbouring trimers in the same membrane layer. The shape of the trimer is approximated by a truncated triangle, especially at the extracellular side of the membrane, and adjacent trimers are separated by a zone of low electron density with a thickness of 10 Å.

In general, repulsive forces as well as attractive forces are necessary to maintain a well ordered crystalline structure (Israerachvili, 1995). The origin of the repulsive force is identified in the present structural analysis. In the honeycomb lattice, Lys172 and Arg175 in the *F* helix are buried deeply in a putative hydrophobic region and have their side chains directed towards the sixfold symmetry axis. That is, the trimers are oriented so as to separate this pair of positively charged residues as far as possible from corresponding pairs in neighbouring trimers. Electrostatic repulsion owing to this uneven distribution of charged amino-acid residues would be

Figure 3
(*a*) Ribbon drawing of the bR monomer (grey) with all-*trans* retinal (purple) and one phospholipid (red). Residues having different orientations from those in the probe model are drawn in green. Residues playing a significant role in maintaining the crystal structure are drawn in orange. The figures were produced using *MolScript* (Kraulis, 1991). (*b*) A helical wheel projection model representing the *A* and *B* helices in one monomer and the *D* and *E* helices in the adjacent monomer. The red circle represents the phosphate group of the lipid found between these helices. Amino-acid residues contacting the phytanyl chains are labelled in black.

expected to be one of the major forces determining the mutual orientation of bR trimers in aggregated states. A similar argument has been given as an explanation of the in-plane orientation of bR trimers in delipidated purple membrane (Grigorieff *et al.*, 1995).

Attractive forces are also required to maintain a crystalline state. It is expected from analysis of the lipid content in the crystal (Takeda *et al.*, 1998) that more than two phospholipids per bR occur in the inter-trimer hydrophobic region. In the difference density map calculated after addition of the immobilized phospholipids in the trimeric structure, a pair of electron-density patches is seen near the twofold symmetry axis in the cytoplasmic membrane leaflet. These patches are likely to arise from phospholipids whose phosphate group can interact with the ε-amino group of Lys30, which protrudes from the *A* helix towards the inter-trimer space (Fig. 3*a*). Since their flexible hydrocarbon chains are able to fill the irregular open space between the hydrophobic amino-acid residues protruding from the transmembrane helical segments, the presence of such lipids in the trimer–trimer interface would be expected to bring about a substantial attractive force between bR trimers.

In addition to the lipid molecules, detergent molecules used for crystallization are also expected to be incorporated into the crystal. Indeed, crystal growth is sensitive to the detergent concentration, and well ordered crystals are produced at a detergent-to-membrane weight ratio of 0.5. Since the miscibility of OTG with the aqueous phase is very low under the crystallization conditions (Takeda *et al.*, 1998), most detergent molecules would be inserted into the hydrophobic region of the membrane layers. This idea explains why the surface area per each trimer is about 1.5 times larger in the honeycomb lattice (4760 Å^2) than in the hexagonal lattice of purple membrane (3370 Å^2). The only possible space which can accommodate a large number of detergent molecules is the inter-trimer region around the sixfold symmetry axis, although their detailed arrangement remains unclear at the present resolution.

The inter-membrane protein–protein interactions impose some restriction on the protein arrangement. However, it is obvious that they cannot fully explain the in-plane orientation of the trimer. Thus, it is concluded that the honeycomb structure is maintained under a balance of protein–protein, protein–lipid and lipid–detergent interactions.

We wish to express our gratitude to all the staff at the Photon Factory, especially Drs N. Sakabe, N. Watanabe, M. Suzuki and N. Igarashi for their help in data collection. This work was supported by grants-in-aid from the Ministry of Education, Science and Culture of Japan, by special coordination funds for Promoting Science and Technology and by research grants to the Biodesign Research Program from RIKEN.

References

Blaulock, A. E. & Stoeckenius, W. (1971). *Nature (London)*, **233**, 152–155.
Brünger, A. T. (1992*a*). *X-PLOR Version* 3.1. *A System for X-ray Crystallography and NMR*. New Haven: Yale University Press.
Brünger, A. T. (1992*b*). *Nature (London)*, **355**, 4772–475.
Casadio, R., Gutowitz, H., Mowery, P., Taylor, M. & Stoeckenius, W. (1980). *Biochim. Biophys. Acta*, **590**, 13–23.
Collaborative Computational Project, Number 4 (1994). *Acta Cryst.* D**50**, 760–763.
Denkov, N. D., Yoshimura, H., Kouyama, T., Walz, J. & Nagayama, K. (1998). *Biophys. J.* **74**, 1409–1420.
Ebrey, T. G. (1993). *Thermodynamics of Membrane Receptors and Channels*, edited by M. Jackson, pp. 353–387. Boca Raton: CRC Press.
Fukuda, K., Ikegami, A., Nasuda-Kouyama, A. & Kouyama, T. (1990). *Biochemistry*, **29**, 1997–2002.
Grigorieff, N., Beckmann, E. & Zelmlin, F. (1995). *J. Mol. Biol.* **254**, 404–415.
Grigorieff, N., Ceska, T. A., Downing, K. H., Baldwin, J. M. & Henderson, R. (1996). *J. Mol. Biol.* **259**, 393–421.
Henderson, R., Baldwin, J. M., Ceska, T. A., Zemlin, F., Beckmann, E. & Downing, K. H. (1990). *J. Mol. Biol.* **213**, 899–929.
Higashi, T. (1989). *J. Appl. Cryst.* **22**, 9–18.
Israerachvili, J. (1995). *Intermolecular and Surface Forces*, 2nd ed. London: Academic Press.
Kates, M., Moldoveanu, N. & Stewart, L. C. (1993). *Biochim. Biophys. Acta*, **1169**, 46–53.
Kimura, N., Vassylyev, D. G., Miyazawa, A., Kidera, A., Matsushima, M., Mitsuoka, K., Murata, K., Hirai, T. & Fujiyoshi, Y. (1997). *Nature (London)*, **389**, 206–211.
Kouyama, T., Yamamoto, M., Kamiya, N., Iwasaki, H., Ueki, T. & Sakurai, I. (1994). *J. Mol. Biol.* **236**, 990–994.
Kraulis, P. (1991). *J. Appl. Cryst.* **24**, 946–950.
Landau, E. M. & Rosenbusch, J. P. (1996). *Proc. Natl Acad. Sci. USA*, **93**, 14532–14535.
Laskowski, R. A., MacArthur, M. W., Moss, D. S. & Thornton, J. M. (1993). *J. Appl. Cryst.* **26**, 283–291.
McRee, D. E. (1993). *Practical Protein Crystallography*. San Diego: Academic Press.
Oesterhelt, D. & Stoeckenius, W. (1974). *Methods Enzymol.* **31**, 667–678.
Otomo, J., Urabe, Y., Tomioka, H. & Sasabe, H. (1992). *J. Microbiol.* **138**, 2389–2396.
Pomerleau, V., Harvey-Girard, E. & Boucher, F. (1995). *Biochim. Biophys. Acta*, **1234**, 221–224.
Sakabe, N. (1983). *J. Appl. Cryst.* **16**, 542–547.
Schertler, G. F., Bartunik, H. D., Michel, H. & Oesterhelt, D. (1993). *J. Mol. Biol.* **234**, 156–164.
Sternberg, B., L'Hostis, C., Whiteway, C. A. & Watts, A. (1992). *Biochim. Biophys. Acta*, **1108**, 21–30.
Stoeckenius, W., Lozier, R. & Bogomolni, R. A. (1979). *Biochim. Biophys. Acta*, **505**, 215–278.
Takeda, K., Sato, H., Hino, T., Kono, M., Fukuda, K., Sakurai, I., Okada, T. & Kouyama, T. (1998). *J. Mol. Biol.* **283**, 463–474.